Carbon Nanotube Reinforced Rigid-Rod Polyimide

Minoo Naebe, Jing Wang, Yuhua Xue, Xungai Wang, Tong Lin

Centre for Material and Fibre Innovation, Deakin University, Geelong VIC 3217, Australia

Received 8 June 2009; accepted 6 March 2010
DOI 10.1002/app.32395
Published online 19 May 2010 in Wiley InterScience (www.interscience.wiley.com).

ABSTRACT: Multiwalled carbon nanotube/rigid-rod polyimide composite films have been prepared by casting a solution of precursor polymer (polyamide acid) containing multiwalled carbon nanotubes (MWNTs) into thin films, followed by a thermal imidization treatment. The composite films were characterized by FTIR, TEM, DSC, TGA and TMA, and the film tensile properties were also examined. The presence of 1.0% MWNTs in the polymer matrix led to more than twofold increase in tensile strength of the rigid-rod polyimide composite films and improved thermal stability, but reduced in thermal deformation. However, the tensile property did not show further increase when the film contained higher composition of MWNTs. © 2010 Wiley Periodicals, Inc. J Appl Polym Sci 118: 359–365, 2010

Key words: polyimide; rigid-rod polymer; carbon nanotubes; composite; mechanical properties; thermal expansion

INTRODUCTION

Poly(*p*-phenylene biphenyltetracarboximide) (BPDA-PDA) is a rigid rod-like polyimide showing many excellent properties such as chemical resistance, thermal stability, mechanical strength and electric insulation because of the highly rigid backbone and ordered molecular arrangement,[1–9] which is similar to other rigid-rod polymers.[10,11] It also has many unique features including low thermal expansion coefficient (CTE), high modulus and very low water diffusion coefficient.[12,13] It has been reported that BPDA-PDA has threefold higher fracture toughness compared to flexible polyimide, poly(4,4′-oxydiphenylene pyromellitimide) (PMDA-ODA).[14] The excellent mechanical properties and thermal stability along with low processing cost have made BPDA-PDA a widely used dielectric insulating material in the integrated circuits.[15,16] Nevertheless, the relatively low flexibility and brittleness[17] could restrict the application of BPDA-PDA in other areas such as gas storage tanks.

It is well established that the properties of a polymeric material are highly affected by nano-sized fillers incorporated into the polymer matrix, which are highly dependent on the type and the dimension of fillers, their dispersion state and the interaction with the hosting polymer matrix. Various nanofillers have been studied with the purposes of improving the mechanical, electronic and thermal properties, increasing the gas barrier ability, and reducing the thermal deformation.[4,12,18,19] Among the fillers studied, carbon nanotubes (CNTs) with a high aspect ratio and low density are considered to be one of the ultimate filler materials that can considerably improve mechanical, electric and thermal properties of polymeric materials incorporated.[20]

Nanocomposites of carbon nanotubes with flexible and semiflexible polyimides such as poly(4,4′-oxydiphenylene pyromellitimide) (PMDA-ODA),[21–25] asymmetric poly(4,4′-oxydiphenylene biphenyltetracarboximide) (a-BPDA-ODA),[26] poly(3,4′-oxydiphenylene biphenyltetracarboximide) (BPDA-ODA),[27] and poly (4,4′-oxydiphenylene benzophenonetetracarboximide) (BTDA-ODA),[28] and a rigid-rod poly (*p*-phenylene benzobisoxazole) (PBO)[29] have been reported. These composite materials showed enhanced mechanical properties and improved electrical conductivity and thermal stability.

Since the rigid and alignment nature of rigid-rod macromolecules,[1–9] the presence of CNTs in a rigid-rod polymer matrix should alter the molecular orientation, leading to changes in its mechanical and thermal properties. However, how carbon nanotubes influence the mechanical properties of rigid-rod BPDA-PDA has not been found in the research literatures. In this article, nanocomposite films of a rigid-rod BPDA-PDA and multiwalled carbon nanotubes (MWNTs) have been prepared and the influence of MWNTs on the morphology, mechanical strength, thermal stability and thermal expansion properties of the BPDA-PDA were examined.

EXPERIMENTAL

Materials and measurements

N,*N*′-dimethylacetamide (DMAc), 3,3′,4,4′-Biphenyltetracarboxylic dianhydride (BPDA) and 1,4-phenyl-

Correspondence to: T. Lin (tongl@deakin.edu.au).

enediamine (PDA) were obtained from Sigma-Aldrich. PDA was purified by sublimation under vacuum before use. MWNTs were provided by CSIRO Materials Science and Engineering and were purified by refluxing in 3*N* HNO_3 for 48 h before use.

Nuclear magnetic resonance (NMR) spectra were taken on a Varian Unity spectrometer. Differential scanning calorimetry (DSC) was performed using DSC 821 (Mettler Toledo) in alternating DSC mode at an underlying heating rate of 10°C/min. Thermogravimetric analysis (TGA) was performed with a Mettler Toledo TGA/STDA851 and tested in air flow at a heating rate of 10°C/min. Thermo mechanical analysis (TMA) was conducted on a Mettler Toledo TMA/STDA840. Thin film samples were directly placed between a 3 mm ball-point probe and sample support (quartz glass). Samples were heated in a nitrogen atmosphere from 25°C to 700°C at a heating rate of 20°C/min. The tensile properties of the cast films were measured with a universal tensile tester (Lloyd), according to ASTM D-882. Wide angle X-ray diffraction (WAXD) was done on a powder diffractometer (Philips 1140/90) with a Cu radiation 1.5406 Å. Fourier Transform Infrared (FTIR) spectra were recorded by a Bruker Vertex 70 FTIR in ATR mode. The spectra were obtained under 64 scans at 4 cm^{-1} resolution. The data were analysed using OPUS version 5.5 software. The transmission electron microscope (TEM) images were taken using a JEOL JEM-2100 electron microscope.

Synthesis of poly(amide acid) (PAA)

Into a 500 mL Heidolph reactor equipped with nitrogen inlet and stirrer, PDA (8.12 g, 75 mmol) and DMAc (140 mL) were added. The mixture was stirred to form a clear solution and cooled down to −15°C. BPDA (22.07 g, 75 mmol) was added to the solution over a period of 15 min with vigorous stirring. The residual BPDA was washed with 4 mL DMAc and added to the reaction solution. The whole mixture was stirred for 3 h at −15°C, 1 h at 0°C, 1 h at 15°C and then allowed to stand overnight at room temperature. A transparent yellow viscous PAA solution was obtained. A nitrogen atmosphere was maintained in the reactor throughout the course of reaction. The PAA was purified by precipitating three times with acetone. The PAA was dried in vacuum at 40°C for 6 h and stored in a desiccator.

^{1}H-NMR (300 MHz, DMSO-D_6, δ ppm): 12.93 (s, 2H, Ar-NH—), 10.44 (s, 2H, Ar-COOH), 8.25-7.96 (m, 4H, ArH), 7.70 (m, 6H, ArH); ^{13}C-NMR (DMSO-D_6, δ ppm): 169.66, 166.68, 141.25, 139.60, 135.21, 130.45, and 119.94.

Preparation of polymer films

The pure PAA films were fabricated by casting PAA solution (20 wt %) in a Teflon mould and dried in a vacuum oven (8 mbar) at 110°C for 3 h. To prepare MWNT/PAA films, MWNTs were first dispersed in DMAc with the aid of ultrasonication. Dried PAA was then dissolved in this solution to form a solution with the concentration of 20 wt % PAA and 1.0–4.5% MWNTs (based on the weight of PAA). The MWNT/PAA solution was ultrasonicated for 2 h to form homogeneous solutions. The blends were then cast into solid films under the same condition as PAA.

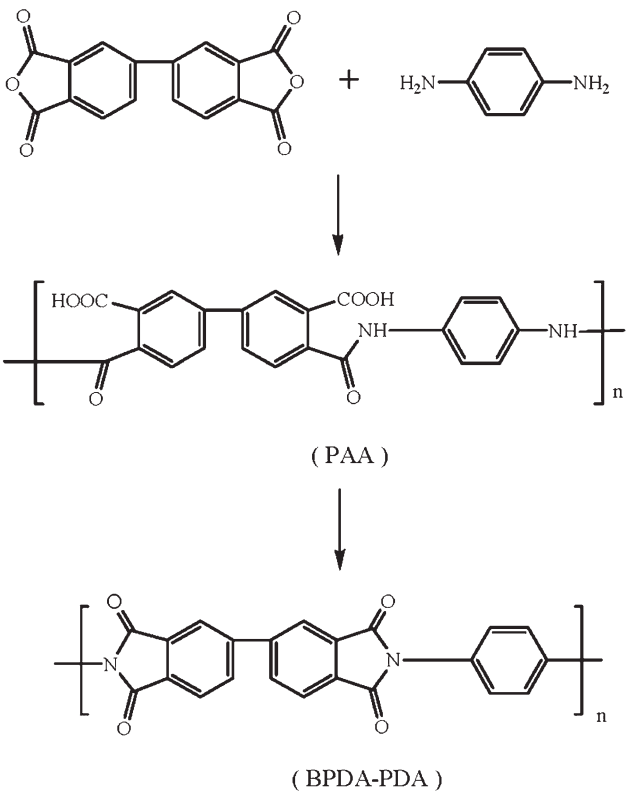

Scheme 1 Synthetic route to the rigid-rod polyimide BPDA-PDA.

The pure PAA and the MWNT/PAA composite films were imidized in a tube furnace under vacuum to produce polyimide films. During imidization, the samples were heated to 300°C (room temperature ~ 200°C, about 3.5°C/min) and finally annealed at 300°C for 2 h.

RESULTS AND DISCUSSION

Synthesis and FTIR spectra

The synthetic route to the rigid-rod polyimide BPDA-PDA is shown in Scheme 1. A polymer precursor, poly(amide acid) (PAA), was synthesized by amidation of the carboxylic anhydrides in BPDA and the amines in PDA at a low temperature to form flexible linear polymer molecules consisting of a carboxylic acid group in each unit. PAA is soluble in DMAc and PAA films can be easily prepared

from PAA-DMAc solution through a film-casting technique. When the PAA films were heated at an elevated temperature, thermal imidization took place between the amide linkage and the adjacent carboxylic acid group, converting PAA to insoluble rigid-rod polyimide, BPDA-PDA. In our study, the imidization process was carried out in vacuum so that the side-product, water, was easier to release from the polymer matrix, and in the meanwhile to avoid any possible thermal degradation. MWNT composite films were produced in a similar method, except that MWNTs were dispersed into the PAA solution before film casting.

Figure 1 shows the FTIR spectra of PAA and BPDA-PDA. Pure PAA displayed the carboxylic acid characteristic vibrations at 1710 cm^{-1} (C=O stretching) and 2900–3200 cm^{-1} (OH stretching). The vibration bands at 1650 cm^{-1} and 1600 cm^{-1} are typical characteristics of amide I peak (C=O stretching) and amide II peak (N—H mixed mode),[30] respectively. The peaks 1560 cm^{-1} and 3200–3300 cm^{-1} correspond to the C—NH stretching and —NH stretching of amides. After the imidization reaction, new peaks at 1770 and 1710 cm^{-1} (typical of imide carbonyl and symmetrical stretching), 1350 cm^{-1} (C—N stretching), and 1120 and 740 cm^{-1} (imide ring deformation)[27,28] appeared in the FTIR spectrum. The presence of carbon nanotubes (concentration up to 4.5%) in the polymer matrix showed very little changes in the FTIR spectrum, presumably due to the low MWNT composition and the weak vibration signals of MWNTs.

Wide angle x-ray diffraction (WAXD)

Both polymer and MWNT/polymer composite samples were characterized by wide angle X-ray diffraction (WAXD). As shown in Figure 2, the WAXD pattern of pure PAA shows a broad peak centred at about $2\theta = 24°$, while the pure BPDA-PDA reveals

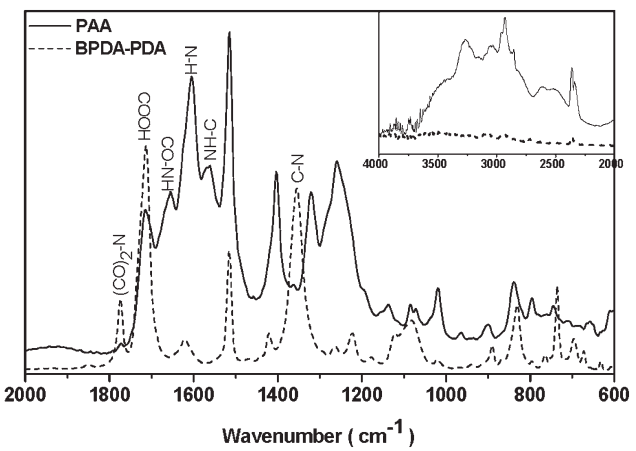

Figure 1 FTIR spectra of PAA and BPDA-PDA.

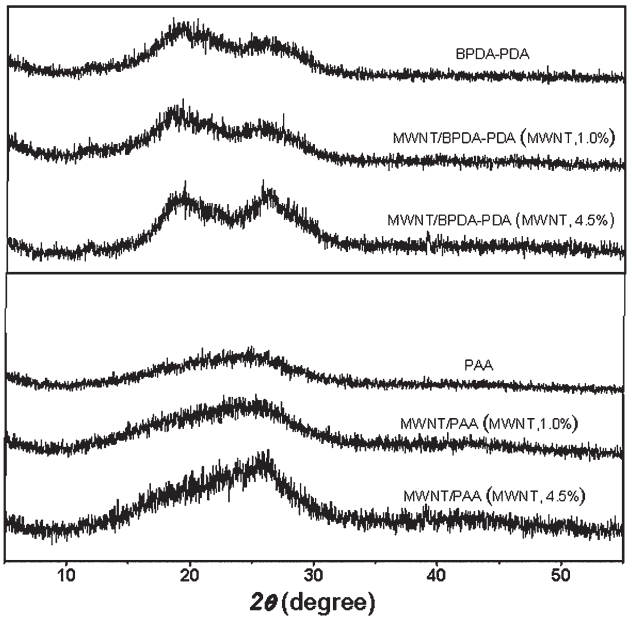

Figure 2 WAXD patterns of PAA and BPDA-PDA films with and without containing MWNTs.

peak reflections at $2\theta = 20°$ and 27°, corresponding to the (200) and (210) reflection planes of the BPDA-PDA, respectively.[1,31,32] For the MWNT composite samples, they showed similar WAXD patterns to the pure polymer samples when the MWNT composition was 1.0%. The reflections at $2\theta = 20°$ and 27° became slightly increased, respectively, when the MWNT composition was increased to 4.5%.

Mechanical properties

The tensile properties of PAA and BPDA-PDA films with and without containing MWNTs are shown in Figure 3(a). For the pure PAA film, the tensile strength and elongation at break were 32.8 MPa and 21.3%, respectively. The imidization treatment increased the tensile strength to 40.1 MPa but the elongation at break decreased slightly to 19.0%, because of the conversion from PAA to rigid-rod polyimide.[33] Incorporation of 1.0% MWNTs into the PAA film increased its tensile strength to 60.4 MPa, which is 84% higher than that of the pure PAA counterpart. The MWNT/BPDA-PDA (MWNTs 1.0%) prepared from the imidization treatment of MWNT-containing PAA film showed considerably increased tensile strength to 126.5 MPa. However, from PAA to BPDA-PDA with the presence of MWNTs in the polymer matrix, the elongation at break just had a very little decrease, from 17.2% to 16.0%. The more than twofold increase in the tensile strength upon adding just 1.0% MWNTs reflected a more pronounced reinforcement effect for the rigid-rod polyimide compared to its precursor.

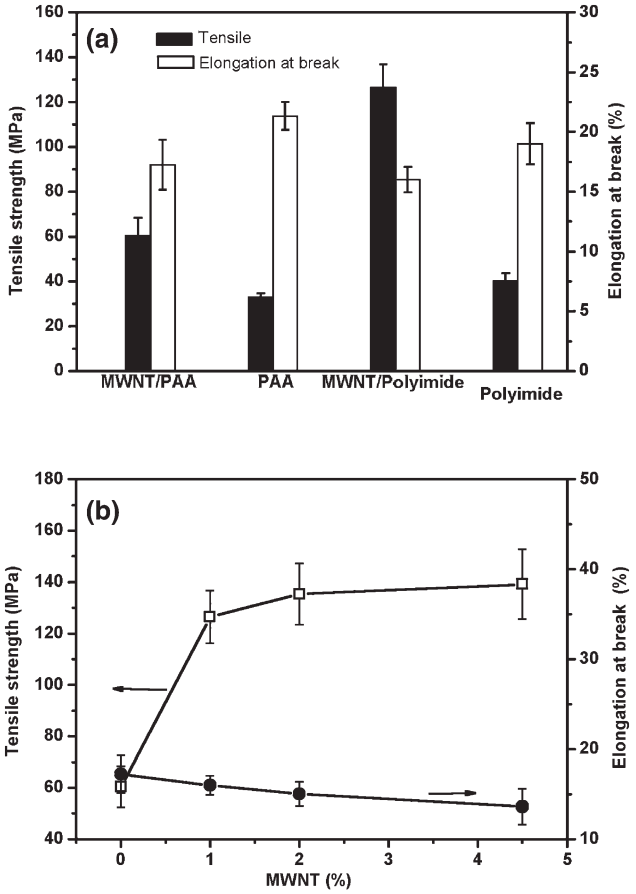

Figure 3 (a) Tensile strength and elongation at break of PAA and BPDA-PDA films with and without containing MWNTs (1.0%), (b) Tensile strength and elongation at break of MWNT/BPDA-PDA with different MWNT compositions.

The effect of MWNT composition on the tensile strength of the BPDA-PDA film is shown in Figure 3(b). With an increase in the MWNT composition from 1.0 to 4.5%, the tensile strength only had a little increase. Such a small improvement in the tensile strength could be attributed to the aggregation effect of nanotubes at a high composition due to strong nanotube-nanotube van der Waals interaction. On the other hand, the elongation at break decreased with the increase in the MWNT composition. The addition of MWNTs to the polymer matrix could restrict the movement of the polymer chains, resulting in lower strain at a higher MWNT composition.

Figure 4 shows TEM images of the sliced MWNT/BPDA-PDA composite samples. When the composition was 1.0% [Fig. 4(a)], MWNTs dispersed uniformly in the BPDA-PDA matrix. Aggregated MWNTs were observed in the composite film containing higher MWNT composition (e.g., 4.5% in Figure 4b). The uneven dispersion and aggregation of carbon nanotubes within the polymer matrix could be the main reason causing reduced improvement rate in tensile strength.

Thermal properties

The DSC thermograms of pure and composite polymer films are shown in Figure 5. For the PAA films, two endothermic peaks with the temperature in ranges of 90–100°C and 170–180°C were observed. The lower endothermic peak corresponds to the evaporation of moisture. The higher endothermic peak includes imidization reaction, heat of decomplexation of poly(amide acid)/solvent and residual solvent evaporation from the polymer matrix.[4,34] The slight exothermic trend at higher temperature (larger than 200°C) can be attributed to rearrangement and ordering of the polymer chains which are caused by the thermal increase in mobility due to the evaporation of residual DMAc solvent. Figure 5(b) shows the DSC thermograms of pure and composite BPDA-PDA films. The disappearance of the imidization peak suggested the completion of the imidization

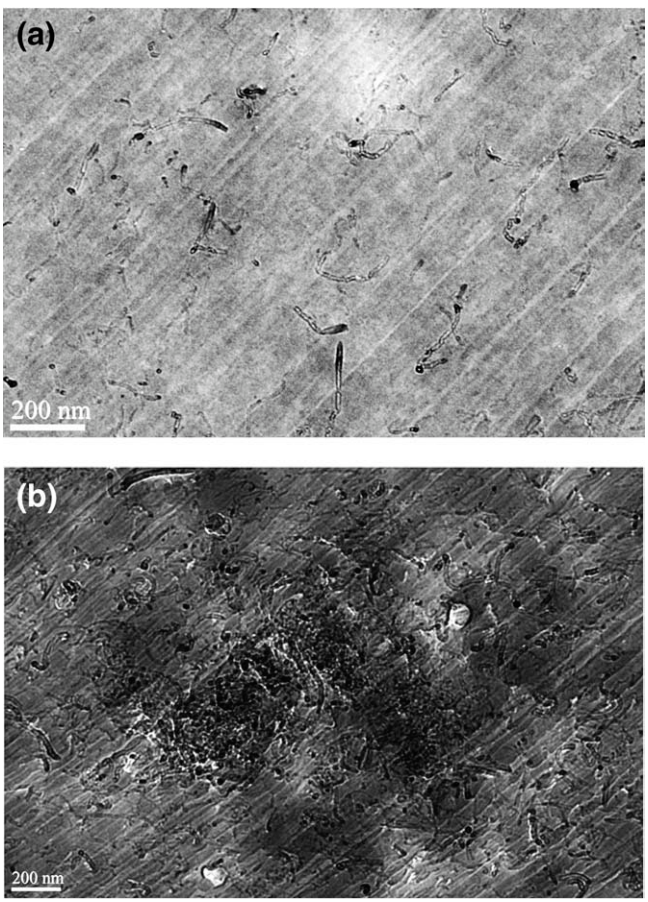

Figure 4 TEM images of polyimide composite film containing (a) 1.0% and (b) 4.5% MWNTs.

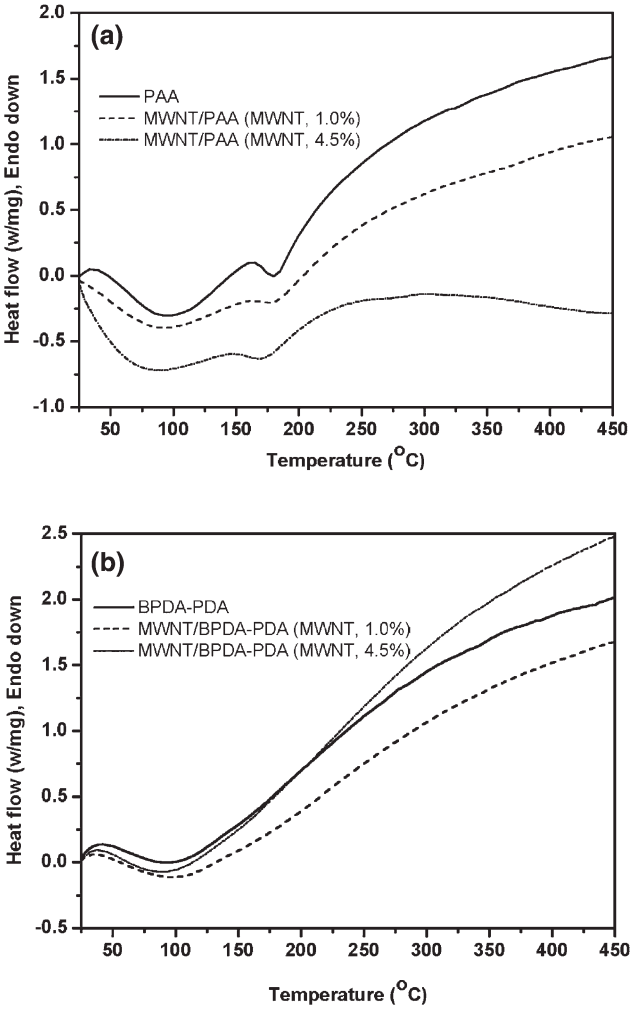

Figure 5 DSC curves of (a) PAA, and (b) BPDA-PDA films.

reaction. Also the moisture peak became broadened indicating more difficulty to evaporate moisture from the polymer matrix. It should be noted that the glass transition temperature (T_g) could not be indentified from the DSC curves.

Figure 6 shows the TGA curves of PAA and BPDA-PDA films. The pure PAA film started to lose weight at about 50°C with a small moisture peak at 105°C. It had three main weight loss derivative peaks (DTG), at 173, 367 and 616°C (Table I). The first two DTG peaks can be attributed to the evaporation of residual DMAc from the cast films and release of moisture due to the imidization reaction. The last one should be associated with the degradation of the polymer. The DTG peaks for the BPDA-PDA film also showed three DTG peaks at about 165, 417 and 619°C. As can be seen from Figure 6(a), the intensity of the first peak was much lower compared to these of the PAA film, due to much less solvent remaining in the polymer matrix.

PAA composite film containing 1.0% MWNTs showed a moisture peak at 99°C with similar weight loss derivative peaks pattern. However, a different thermal degradation process for the MWNT/BPDA-PDA film was observed. The BPDA-PDA composite film only displayed two weight loss peaks around 135°C and 623°C. It was clearly observed that the onset of degradation temperature was significantly higher for the MWNT/BPDA-PDA) (533°C) than that of pure BPDA-PDA (394°C). This suggested that

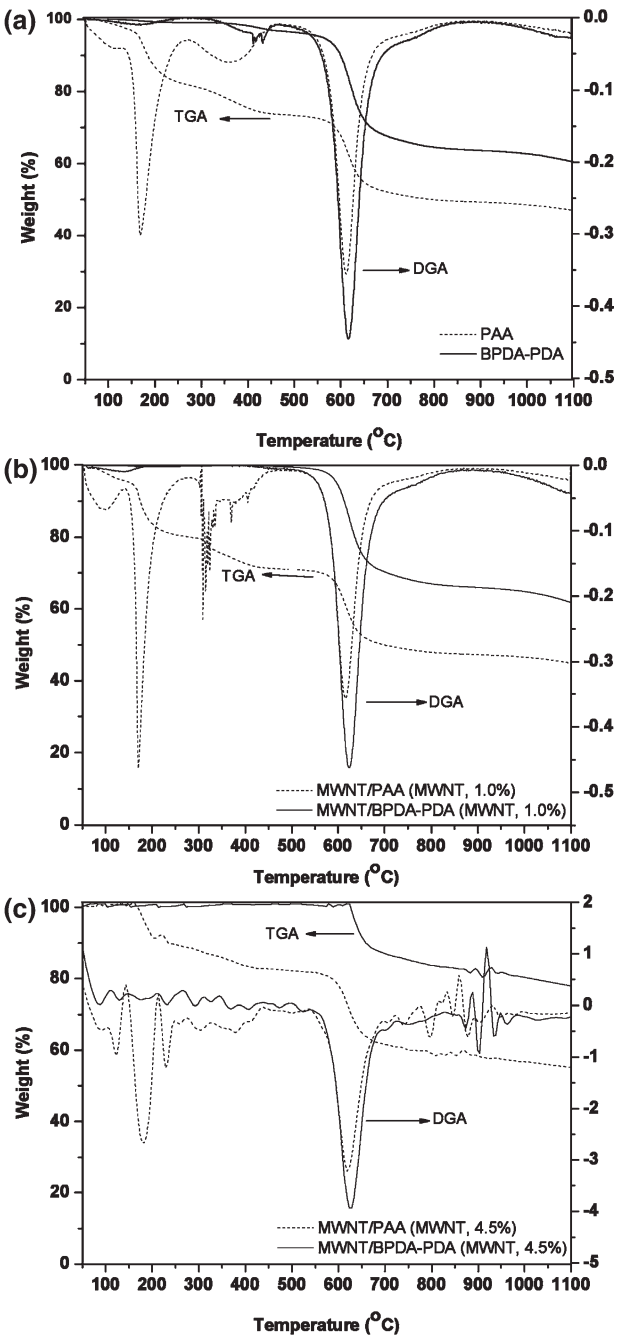

Figure 6 TGA curves of (a) PAA and BPDA-PDA films containing no MWNTs, (b) PAA and BPDA-PDA films containing 1.0% MWNTs, (c) PAA and BPDA-PDA films containing 4.5% MWNTs.

TABLE I
Onsets and Peaks of Weight Loss in TGA Curves, Calculated T_g Value and CTE at 25°C

Samples	1st Peak		2nd Peak		3rd Peak		Calculated T_g (°C)	CTE @ 25°C (10^{-6}°C^{-1})
	Onset (°C)	Peak (°C)	Onset (°C)	Peak (°C)	Onset (°C)	Peak (°C)		
PAA	139	173	278	367	475	616	157	−130
Polyimide	50	165	394	417	475	619	340	−227
MWNT/PAA (MWNT, 1.0%)	139	170	278	309	520	615	158	−27
MWNT/Polyimide (MWNT, 1.0%)	50	135	–	–	533	623	333	−123

the presence of only 1.0% carbon nanotubes improved thermal stability of the rigid-rod polyimide. The MWNT/BPDA-PDA film containing 4.5% nanotubes led to one major weight loss peak at 629°C [Fig. 6(c)]. Compared to the pure BPDA-PDA and the MWNT/BPDA-PDA containing 1.0% MWNTs, the higher MWNT composition led to higher thermal degradation temperature indicating improved thermal stability.

Despite the difficulty in obtaining T_g from the DSC curves, it was easier to calculate the T_g based on the thermal mechanical analysis (TMA).[35] Table I also lists the calculated T_g values for different samples. The pure and composite PAA films had almost the same T_g value, which is about half of the value of the BPDA-PDA counterparts. The T_g of the MWNT/BPDA-PDA film) (333°C) was slightly lower than that of the pure BPDA-PDA film (340°C). The lower T_g value indicated the improved thermal transfer efficiency of the composite sample.

Coefficient of thermal expansion (CTE) of the polymer films can be calculated through thermal mechanical analysis (TMA). The thermal expansion (α) of a material at constant pressure was computed according to eq (1)[36]:

$$\alpha = \frac{1}{L_o}\frac{\partial L}{\partial T} \tag{1}$$

where $\partial L/\partial T$ is the change rate of the sample length with temperature, and L_o is the initial sample length. The dependence of CTE value on temperature based on the TMA curves is shown in Figure 7, and the CTE values at 25°C are listed in Table I. Polyimide usually possesses lower CTE value than other polymers, and the CTE for rigid-rod polyimides is lower than other type of polyimides.[12] The addition of MWNTs to the BPDA-PDA decreased the CTE values when the temperature was low (less than 151°C). Compared to the pure BPDA-PDA film, MWNT/BPDA-PDA composite film had about 55% reduction in the CTE value, suggesting smaller thermal deformation when MWNTs was dispersed in the BPDA-PDA matrix. At higher temperature, however, the CTE for the MWNT/BPDA-PDA composite film showed higher value than that of the pure BPDA-PDA film. The negative CTE values below T_g suggested the thermal shrinkage of the polymer samples.

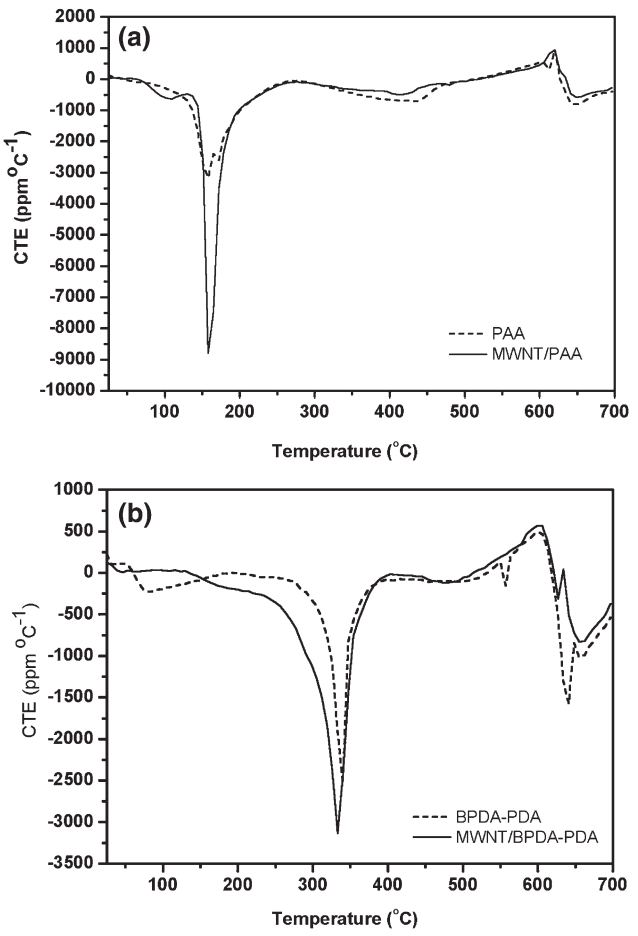

Figure 7 CTE ~ temperature curves of (a) PAA, and (b) BPDA-PDA films.

CONCLUSION

We have demonstrated that the addition of a small amount of multiwall carbon nanotubes (MWNTs) to a rigid-rod polyimide can considerably improve its tensile strength, but the elongation at break does not change much. The presence of MWNTs in the

polymer matrix increases thermal stability and reduces the thermal deformation of the polymer films. However, higher carbon nanotube composition in the rigid-rod polymer matrix does not result in stronger reinforcement to the polymer due to uneven dispersion of MWNTs in the polymer matrix.

The authors thank Dr. Wendy Tian from CSIRO Molecular and Health Technologies for her help with thermal mechanical analysis.

References

1. Ree, M.; Park, Y.-H.; Kim, K.; Kim, S. I.; Cho, C. K.; Park, C. E. Polymer 1997, 38, 6333.
2. Sroog, C. E. Prog Polym Sci 1991, 16, 561.
3. Sroog, C. E. J Polym Sci Macromol Rev 1976, 11, 161.
4. Agag, T.; Koga, T.; Takeichi, T. Polymer 2001, 42, 3399.
5. Jenkins, S.; Jacob, K. I.; Polk, M. B.; Kumar, S.; Dang, T. D.; Arnold, F. E. Macromolecules 2000, 33, 8731.
6. Klop, E. A.; Lammers, M. Polymer 1998, 39, 5987.
7. Tomlin, D. W.; Fratini, A. V.; Hunsaker, M.; Adams, W. W. Polymer 2000, 41, 9003.
8. Wellman, M. W.; Adams, W. W.; Wolff, R. A.; Wiff, D. R.; Fratini, A. V. Macromolecules 1981, 14, 935.
9. Welsh, W. J.; Bhaumik, D.; Mark, J. E. Macromolecules 1981, 14, 947.
10. Hu, X. D.; Jenkins, S. E.; Min, B. G.; Polk, M. B.; Kumar, S. Macromol Mater Eng 2003, 288, 823.
11. Chae, H. G.; Kumar, S. J Appl Polym Sci 2006, 100, 791.
12. Numata, S.; Kinjo, N. Polym Eng Sci 1988, 28, 906.
13. Seo, J.; Han, H. Polym Degrad Stab 2002, 77, 477.
14. Ho, P. S.; Poon, T. W.; Leu, J. J Phys Chem Solids 1994, 55, 1115.
15. Diao, J.; Hess, D. W. Thin Solid Films 2005, 483, 226.
16. Liou, H. C.; Ho, P. S.; Stierman, R. Thin Solid Films 1999, 339, 68.
17. Huang, J. C.; Zhu, Z. K.; Yin, J.; Zhang, D. M.; Qian, X. F. J Appl Polym Sci 2001, 79, 794.
18. Yano, K.; Usuki, A.; Okada, A. J Polym Sci A:Polym Chem 1997, 35, 2289.
19. Herminghaus, S.; Boese, D.; Yoon, D. Y.; Smith, B. A. Appl Phys Lett 1991, 59, 1043.
20. Baughman, R. H.; Zakhidov, A. A.; Heer, W. A. Science 2002, 297, 787.
21. Chou, W.-J.; Wang, C.-C.; Chen, C.-Y. Compos Sci Technol 2008, 68, 2208.
22. So, H. H.; Cho, J. W.; Sahoo, N. G. Eur Polym J 2007, 43, 3750.
23. Chou, W.-J.; Wang, C.-C.; Chen, C.-Y. Polym Degrad Stab 2008, 93, 745.
24. Zhu, B.-K.; Xie, S.-H.; Xu, Z.-K.; Xu, Y.-Y. Compos Sci Technol 2006, 66, 548.
25. Jiang, X.; Bin, Y.; Matsuo, M. Polymer 2005, 46, 7418.
26. Ogasawara, T.; Ishida, Y.; Ishikawa, T.; Yokota, R. Compos Part A 2004, 35, 67.
27. Saeed, M. B.; Zhan, M.-S. Int J Adhes Adhesives 2007, 27, 306.
28. Yuen, S.-M.; Ma, C.-C. M.; Lin, Y.-Y.; Kuan, H.-C. Compos Sci Technol 2007, 67, 2564.
29. Kumar, S.; Dang, T. D.; Arnold, F. E.; Bhattacharyya, A. R.; Min, B. G.; Zhang, X.; Vaia, R. A.; Park, C.; Adams, W. W.; Haughe, R. H.; Smalley, R. E.; Ramesh, S.; Willis, P. A. Macromolecules 2002, 35, 9039.
30. Yang, S. Y.; Rubner, M. F. J Am Chem Soc 2002, 124, 2100.
31. Ree, M.; Chen, K.-J.; Kirby, D. P.; Katzenellenbogen, N.; Grischkowsky, D. J Appl Phys 1992, 72, 2014.
32. Ree, M.; Chu, C. W.; Goldberg, M. J. J Appl Phys 1994, 75, 1410.
33. Chung, H.; Joe, Y.; Han, H. J Appl Polym Sci 1999, 74, 3287.
34. Wang, S.; Liang, Z.; Gonnet, P.; Liao, Y. H.; Wang, B.; Zhang, C. Adv Funct Mater 2007, 17, 87.
35. Qiu, J.; Zhang, C.; Wang, B.; Liang, R. Nanotechnology 2007, 18, 275708.
36. Philip, B.; Xie, J. Smart Mater Structures 2004, 13, 295.